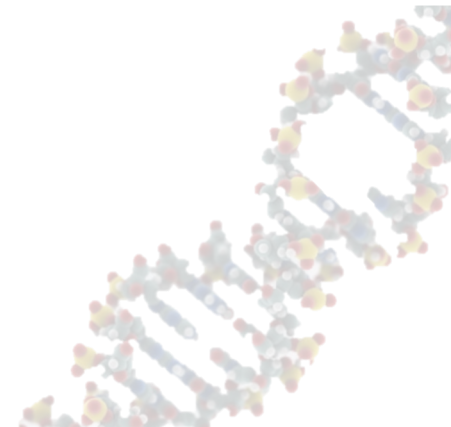
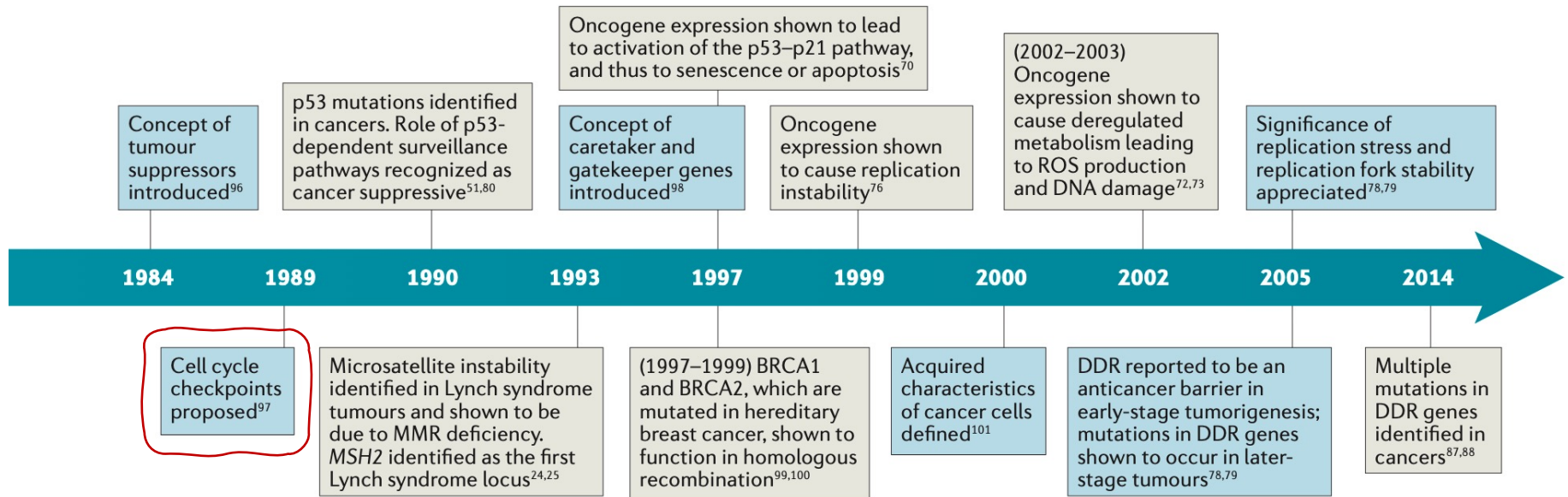




CHECKPOINT DA DANNO AL DNA

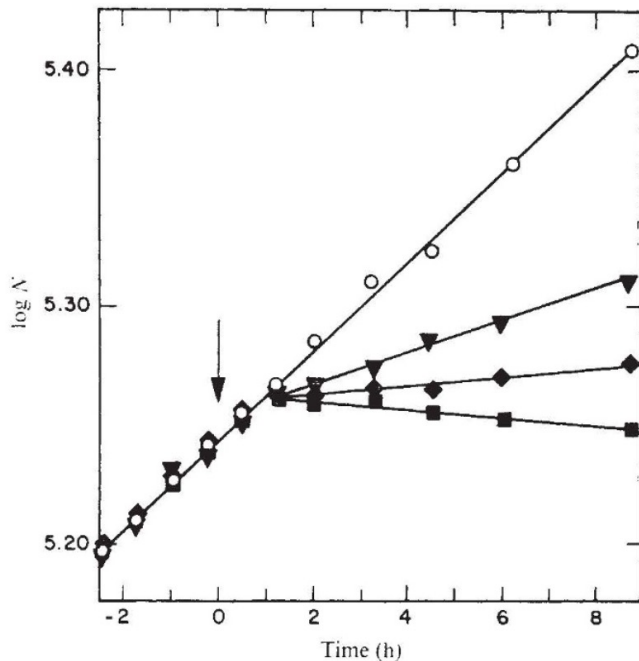
Instabilità genetica e danno al DNA



Identificazione del checkpoint da danno

Trattamento con Neocarzinostatina di cellule di criceto arresta le crescita delle cellule in G2.

Fig. 1 Determination of the terminal point of action of neocarzinostatin in line CHO Chinese hamster cells. A culture of exponentially growing CHO cells in F-10 medium, supplemented with 10% calf serum and 5% foetal calf serum, was split into four subcultures. At time zero, one culture received no drug and served as the control (○). Neocarzinostatin was added to the other cultures, yielding final concentrations of 50 $\mu\text{g ml}^{-1}$ (▲), 400 $\mu\text{g ml}^{-1}$ (◆), or 1,000 $\mu\text{g ml}^{-1}$ (■). Cells were counted at hourly intervals with an electronic cell counter.



Contenuto di DNA in cell wt e AT in risposta a raggi X.

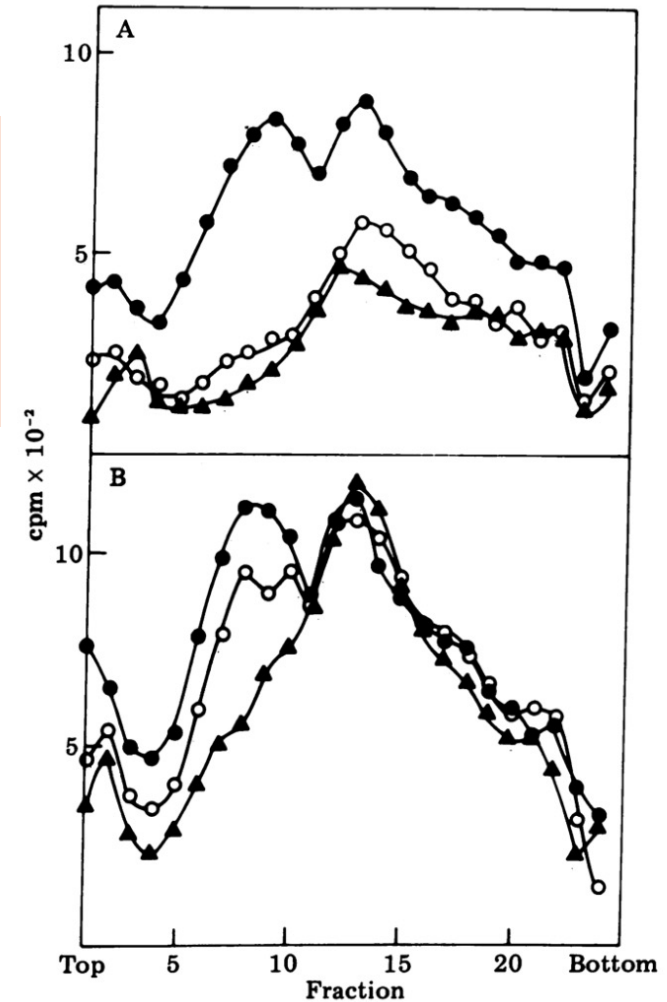


FIG. 2. Alkaline sucrose gradient profiles of the DNA (labeled in a 10-min pulse) of E-11 normal diploid cells (A) and AT cells (B) 30 min after irradiation with 2000 (▲), 500 (○), or 0 (●) rad of x-rays. Relative rates of DNA synthesis for normal diploids were 52% of control after 500 rad and 40% of control after 2000 rad; for AT cells, the relative rates of DNA synthesis were 94% of control after 500 rad and 80% of control after 2000 rad.

Identificazione del primo gene di checkpoint

The *RAD9* Gene Controls the Cell Cycle Response to DNA Damage in *Saccharomyces cerevisiae*

TED A. WEINERT AND LELAND H. HARTWELL

Cell aploidi di lievito raggi X.

wt untreated

IR

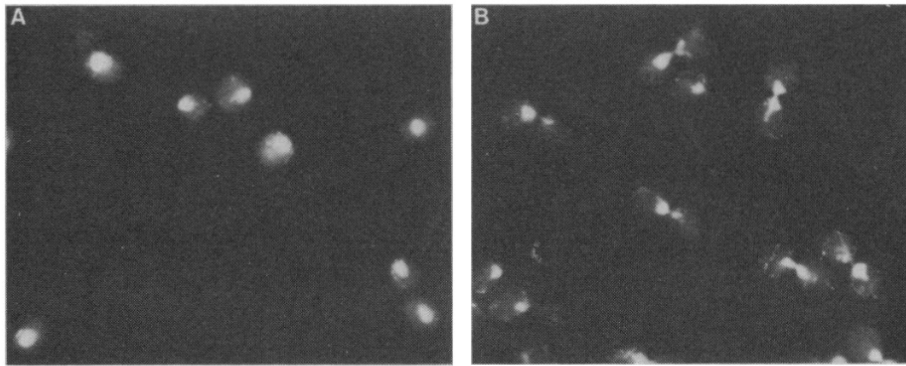


Fig. 2. Nuclear morphology of logarithmically growing and G2-arrested cells. Haploid cells grown to logarithmic phase were either fixed directly or plated on solid agar medium, irradiated with 2 krad, incubated for 3 hours at 23°C, then recovered and fixed. Nuclei were visualized by staining with 4,6-diamino-2-phenylindole (31) and photographed by fluorescence microscopy. (A) *RAD9+* logarithmically growing; (B) *RAD9+* irradiated with 8 krad.

Untreated

IR

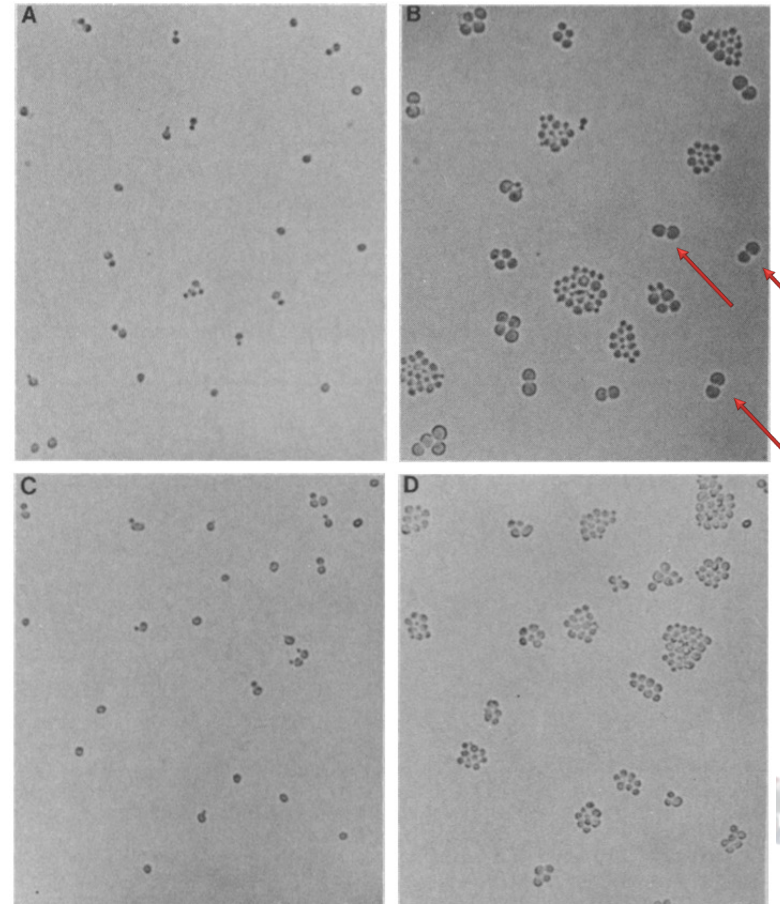


Fig. 3. Photomicroscopy of irradiated *RAD9+* and *rad9* cells. Haploid yeast cells grown to logarithmic phase were plated on thin agar slabs, x-irradiated with 2 krad, and protected from drying with a glass cover slip. Fields of cells were photographed by phase contrast microscopy at the time of irradiation (A and C) and after a 10-hour incubation at 23°C (B and D). Fields were selected and aligned to demonstrate the fate of individual unbudded and large budded cells. (A and B) *RAD9+*; (C and D) *rad9*.

Il checkpoint da danni la DNA

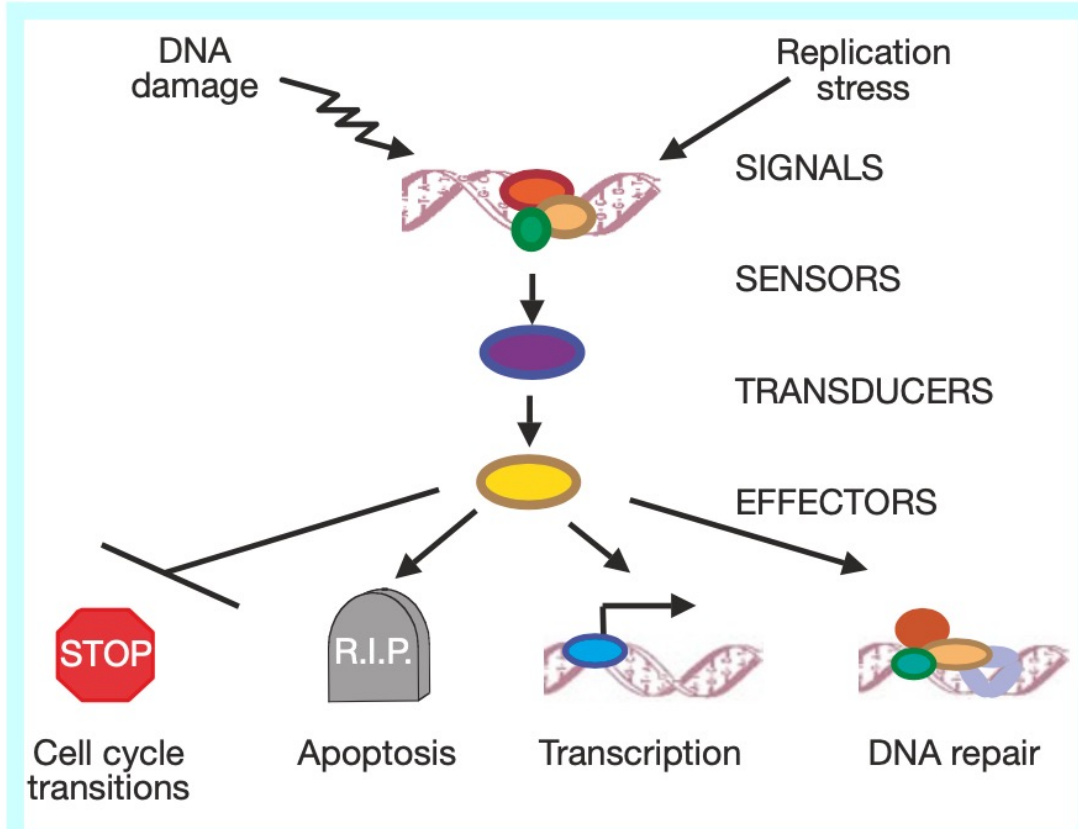
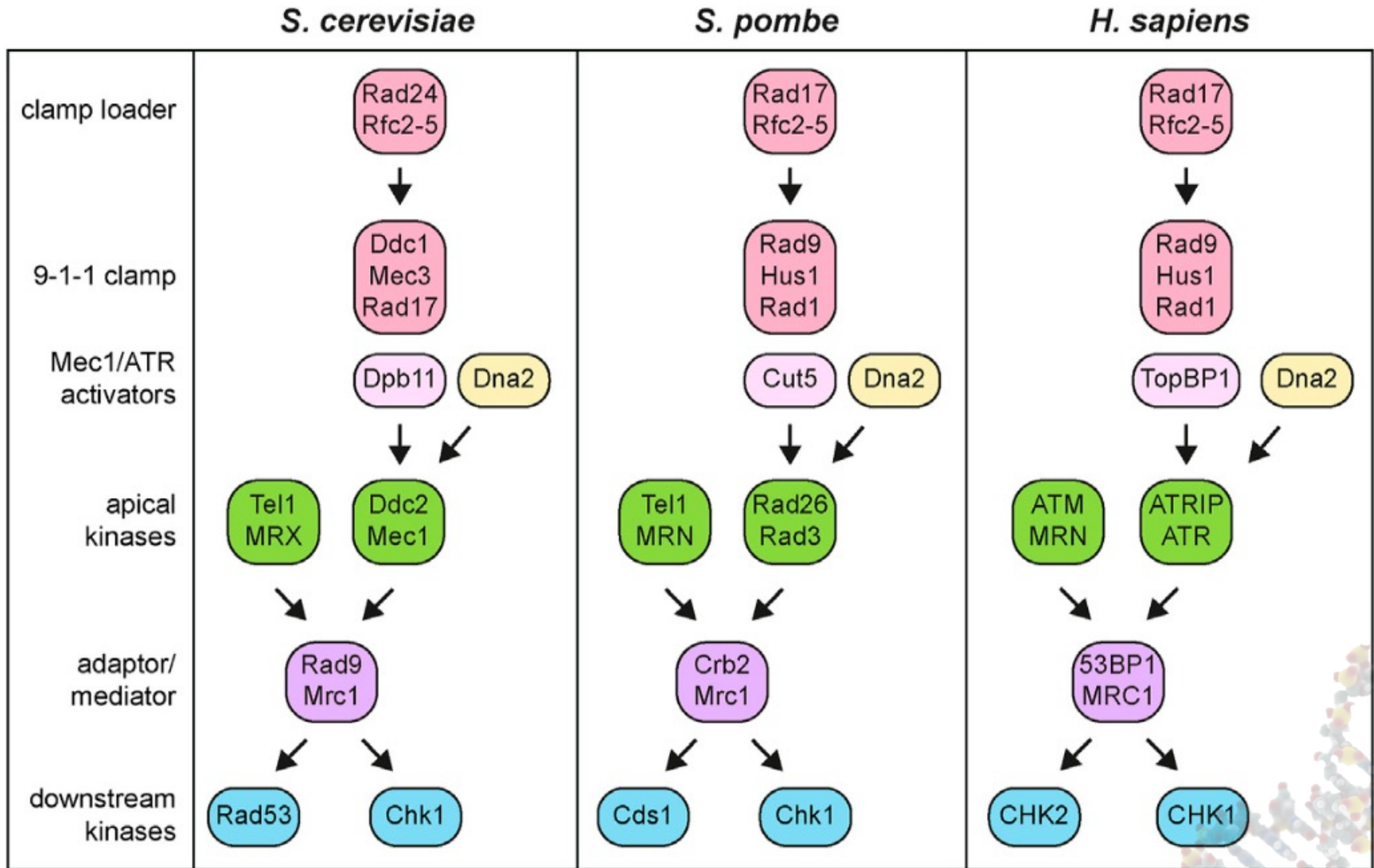
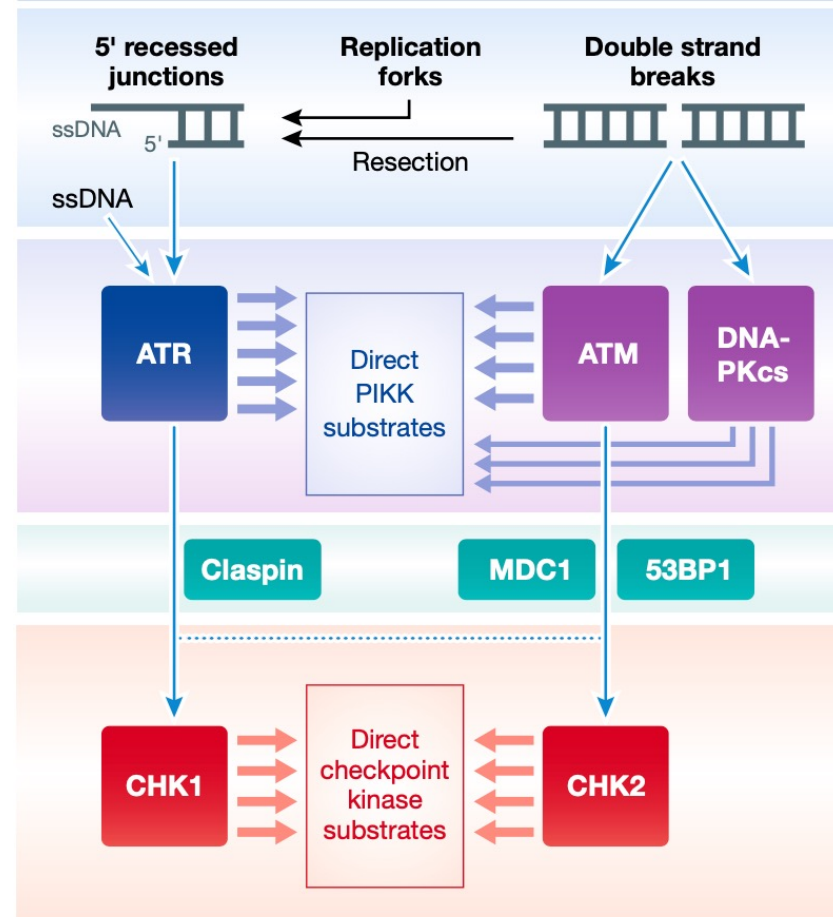
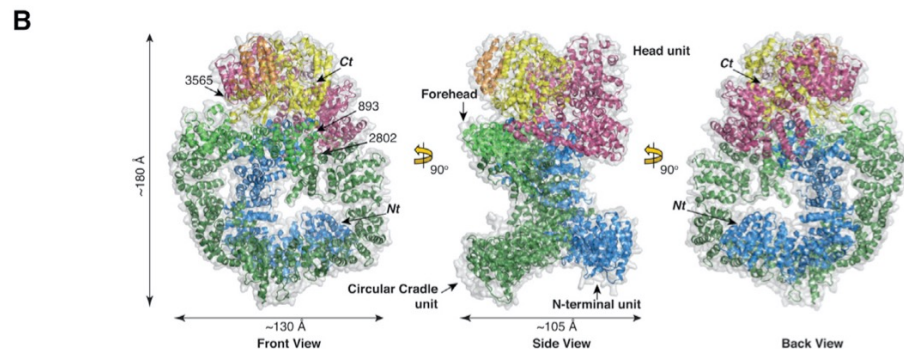
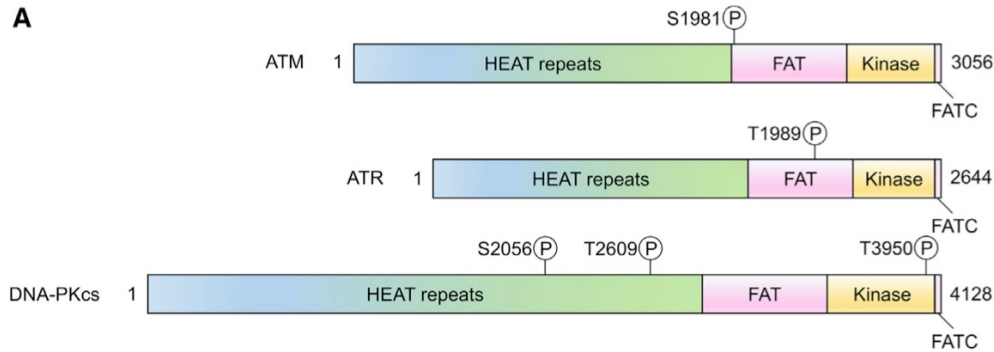


Figure 1 A contemporary view of the general outline of the DNA damage response signal-transduction pathway. Arrowheads represent activating events and perpendicular ends represent inhibitory events. Cell-cycle arrest is depicted with a stop sign, apoptosis with a tombstone. The DNA helix with an arrow represents damage-induced transcription, while the DNA helix with several oval-shaped subunits represents damage-induced repair. For the purpose of simplicity, the network of interacting pathways are depicted as a linear pathway consisting of signals, sensors, transducers and effectors.

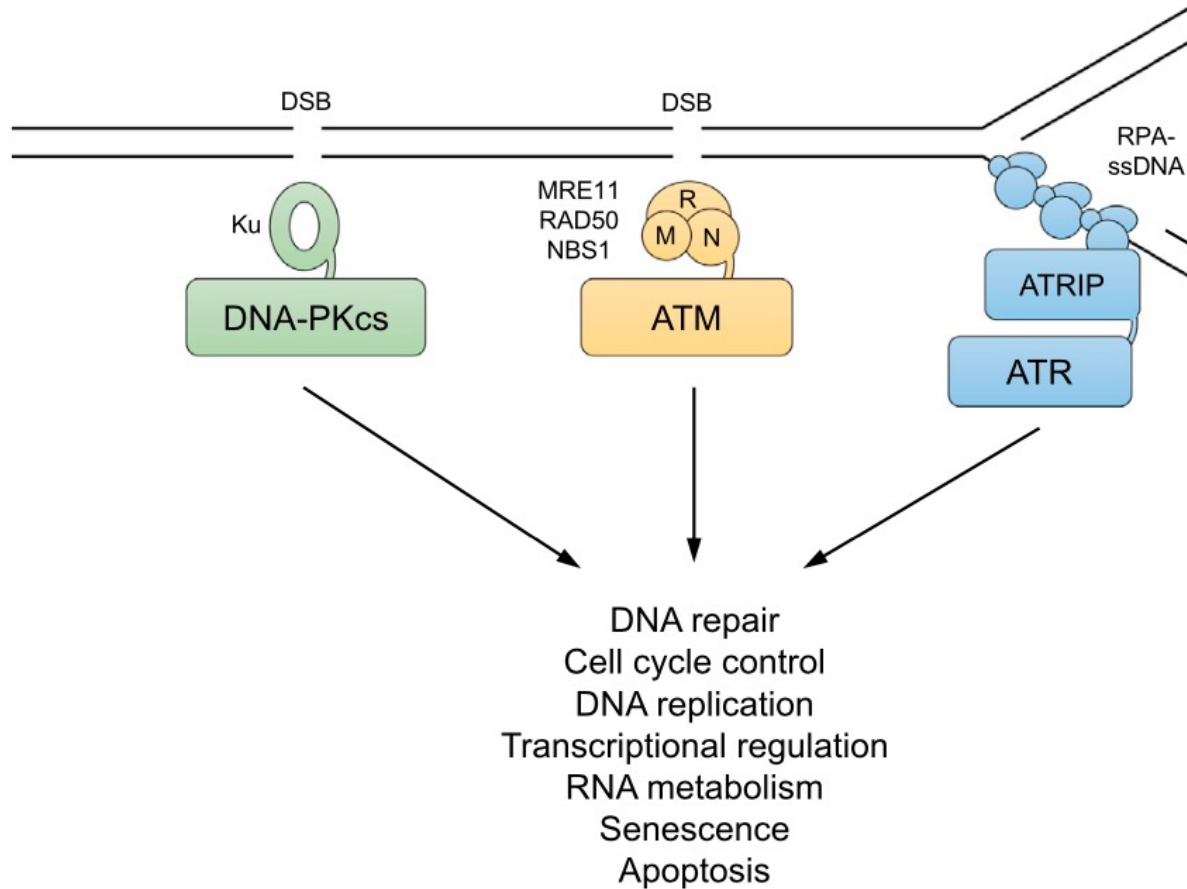
Principali geni di checkpoint conservati



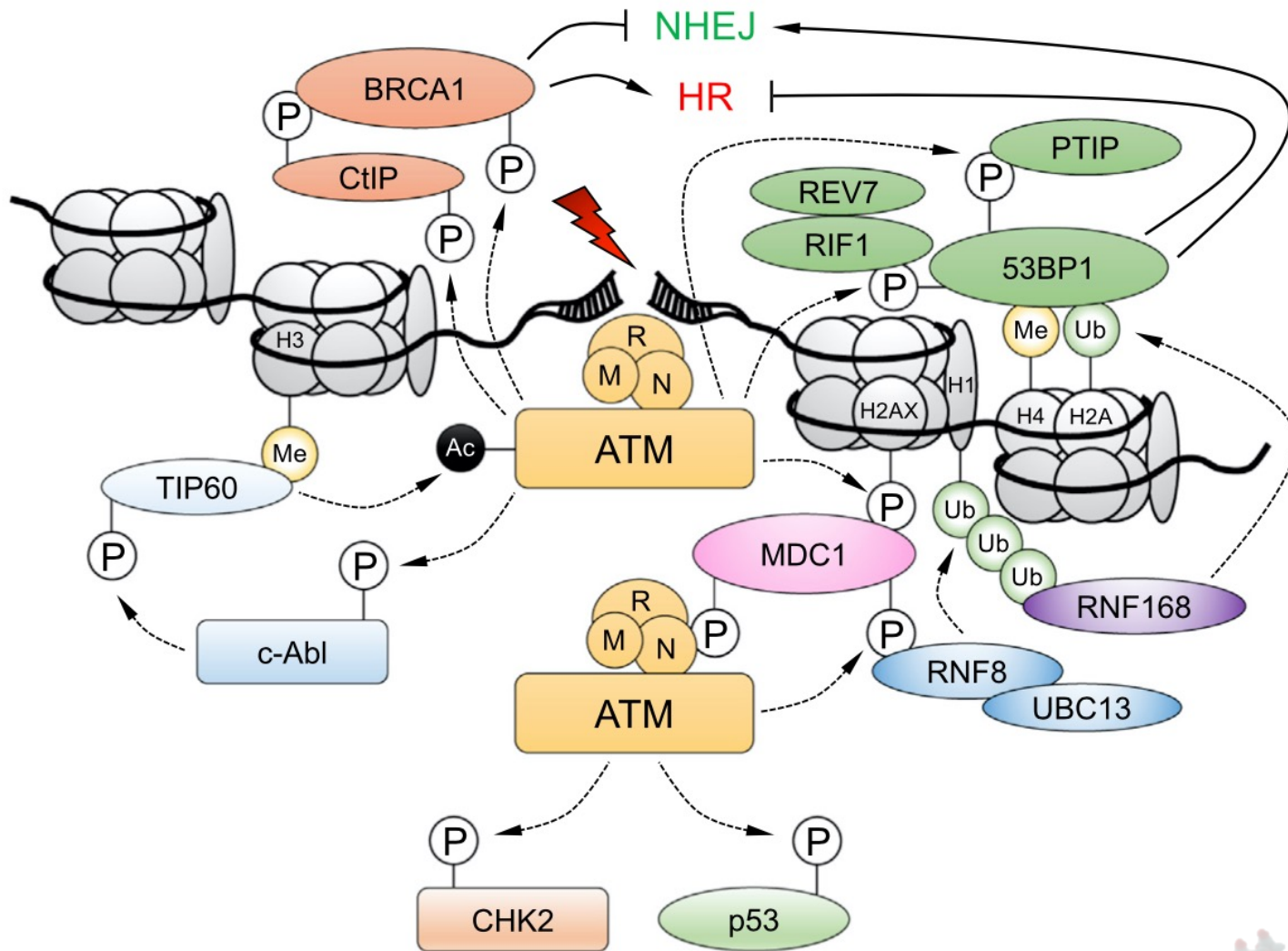
Le chinasi di checkpoint



Le chinasi di checkpoint



ATM activation



ATR activation

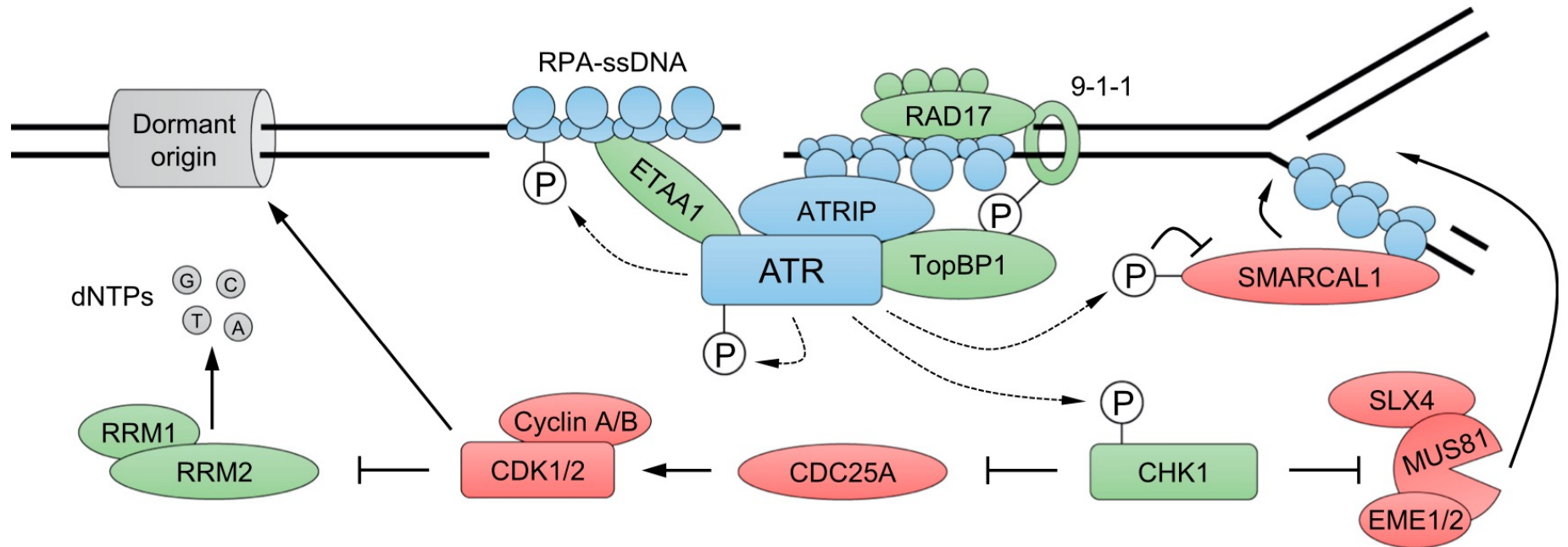


Figure 5. ATR Recruitment and Activation of S Phase Checkpoint Signaling

ATR is recruited to RPA-ssDNA and activated by TopBP1 or ETAA1. ETAA1 is recruited directly to RPA-coated ssDNA. TopBP1 is recruited via mechanisms that are not yet clear, but its role in ATR activation requires interaction with the RAD9-HUS1-RAD1 (9-1-1) clamp complex, which is loaded onto ds/ssDNA junctions by the RAD17/RFC2-5 clamp loader. ATR signaling activates the CHK1 kinase and restrains fork processing enzymes such as SMARCAL1. CHK1 activation causes CDC25A degradation, leading to inhibition of CDK activity, slowing of cell-cycle progression, inhibition of late-origin firing, and increased nucleotide availability, in part by upregulation of RRM2. ATR and its recruitment factors are shown in blue. Factors with a positive role in ATR stimulation or that are activated by ATR are in green, while those that are inhibited by ATR are in red. See text for further details.

DNA-PK and NHEJ

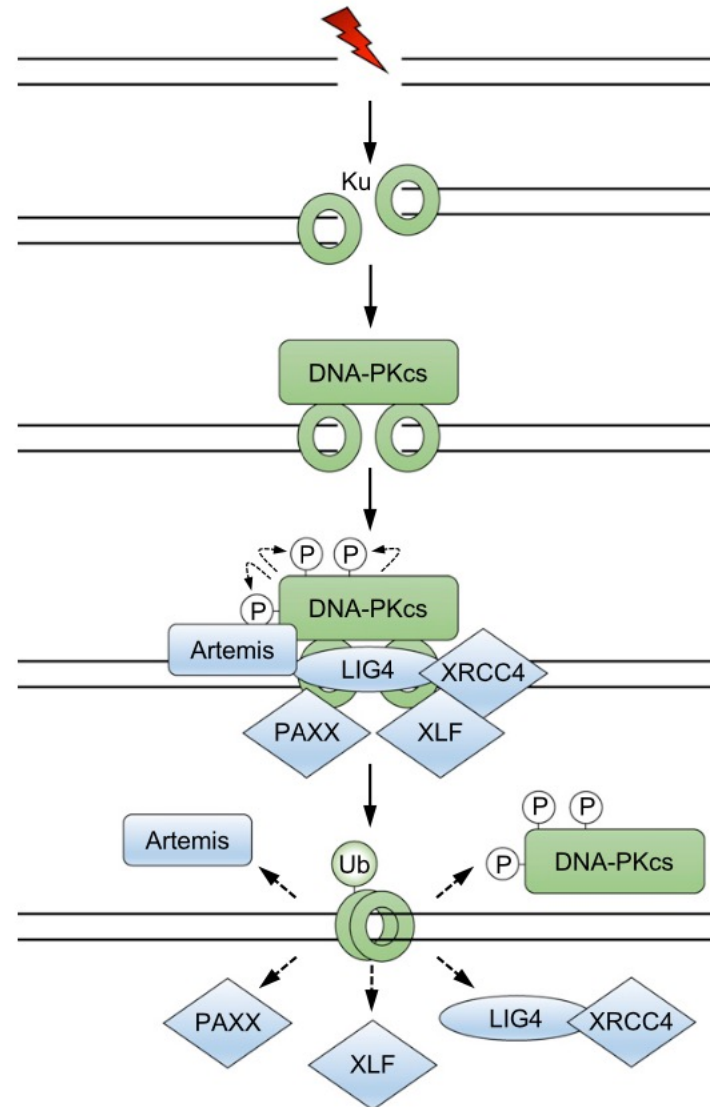
Step 1: DSB induction

Step 2: Ku loading

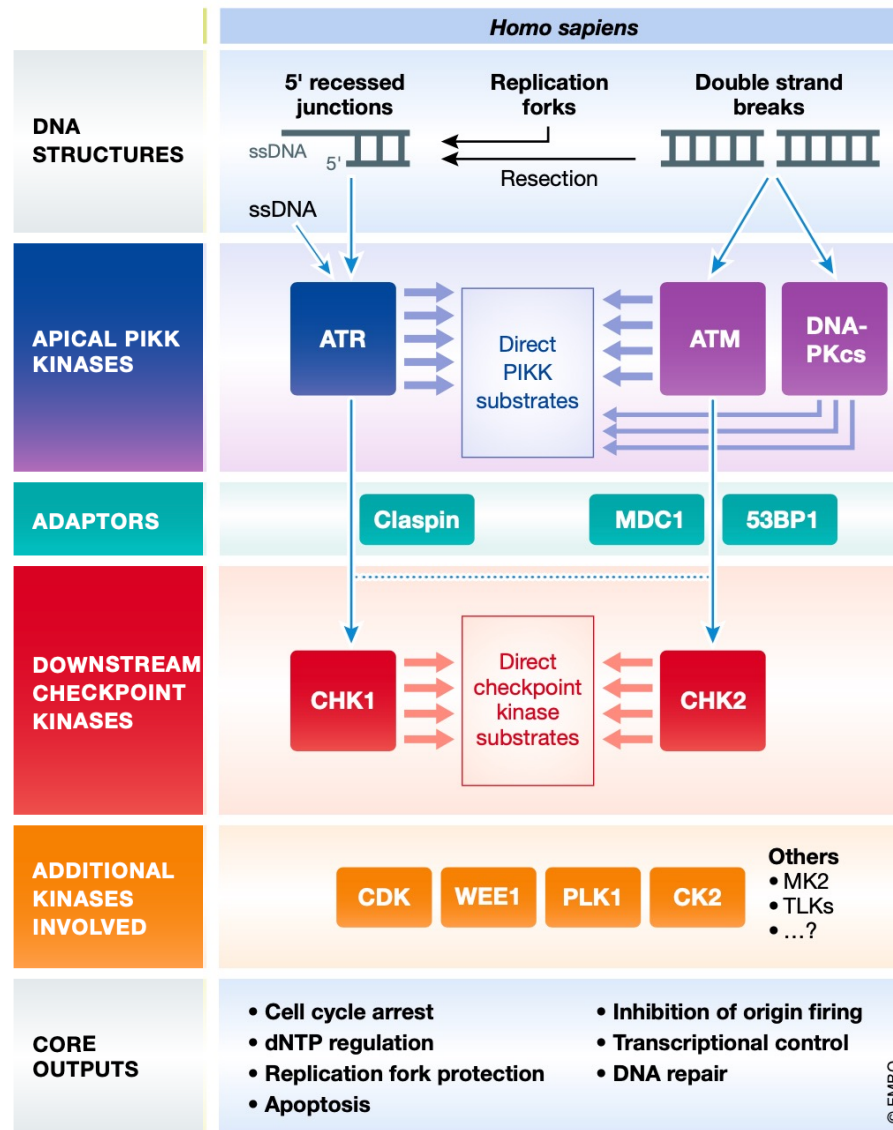
Step 3: DNA-PKcs recruitment
& long-range DNA end synapsis

Step 4: Recruitment of downstream NHEJ
core factors, DNA-PKcs phosphorylation
& short-range DNA-end synapsis

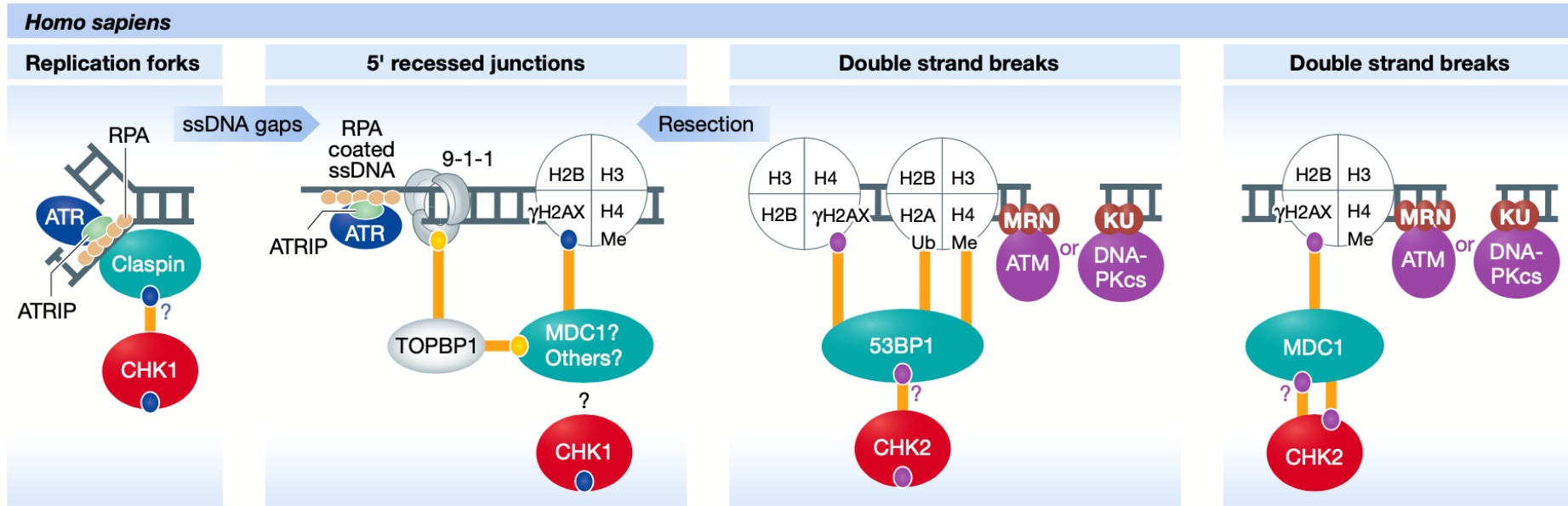
Step 5: DNA-end ligation
& NHEJ complex disassembly



Le chinasi di checkpoint



Attivazione delle protein chinasi downstream



Kinase responsible for phosphorylation

H. sapiens

● ATR

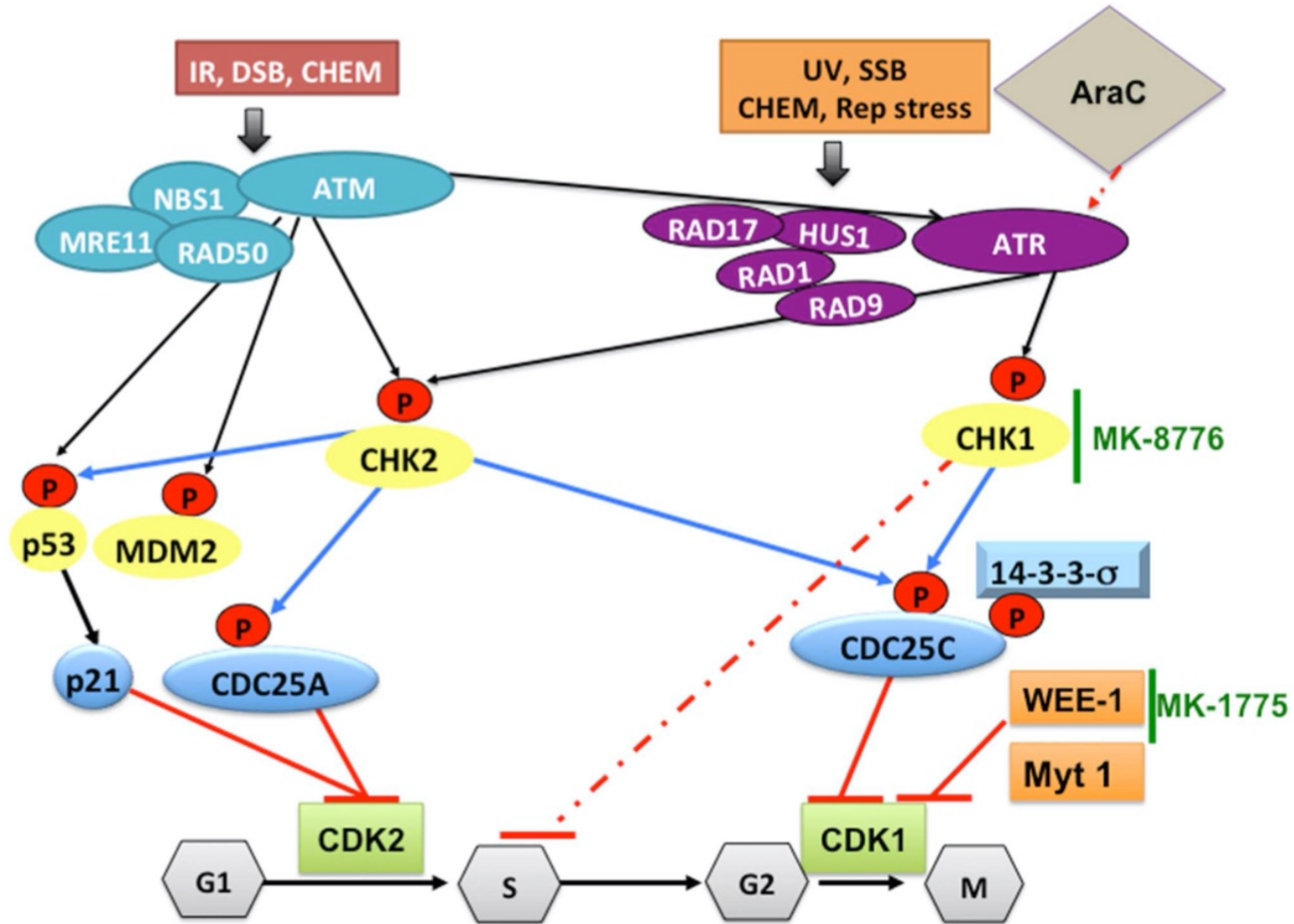
● ATM

● CDK

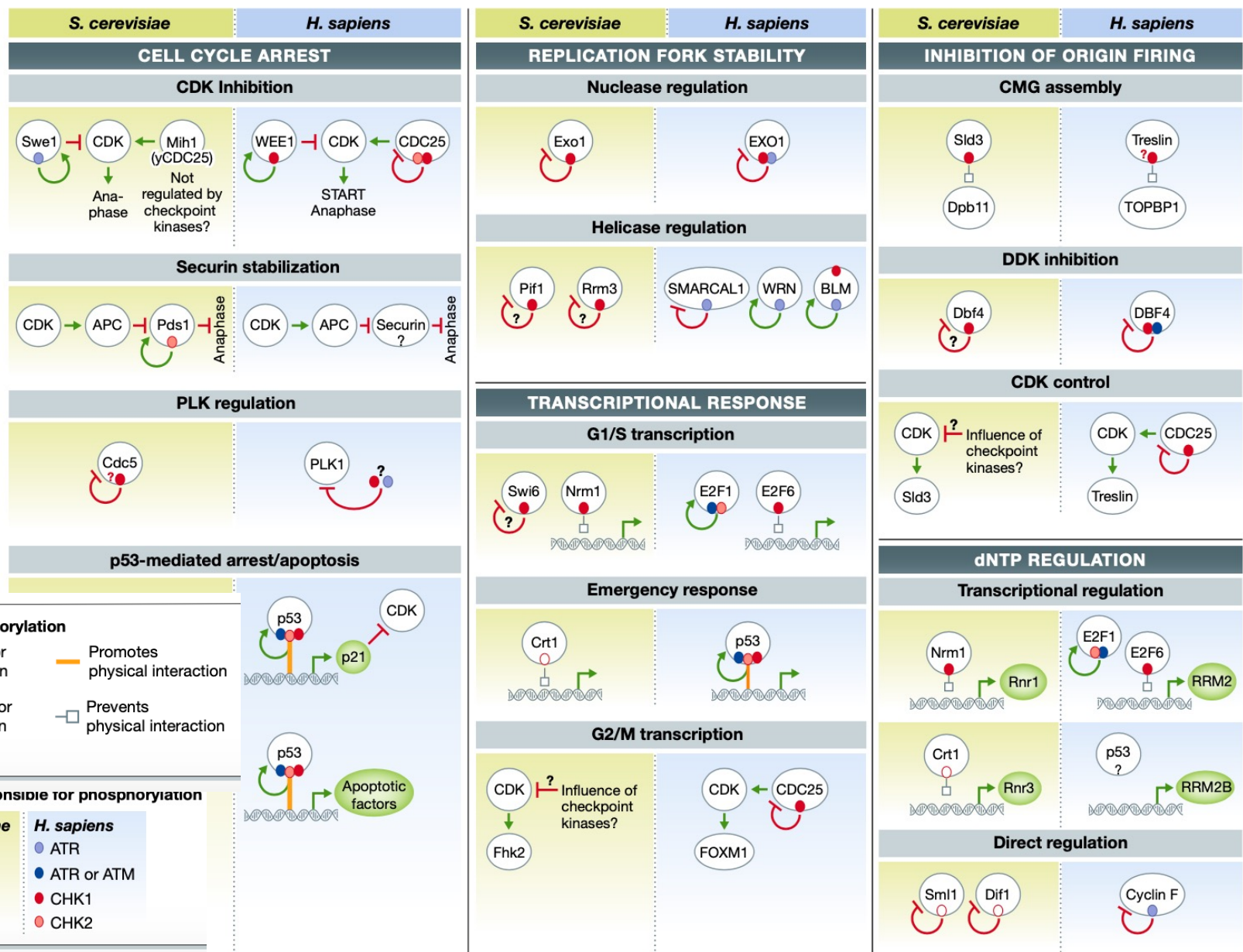
● CK2

— Physical interaction

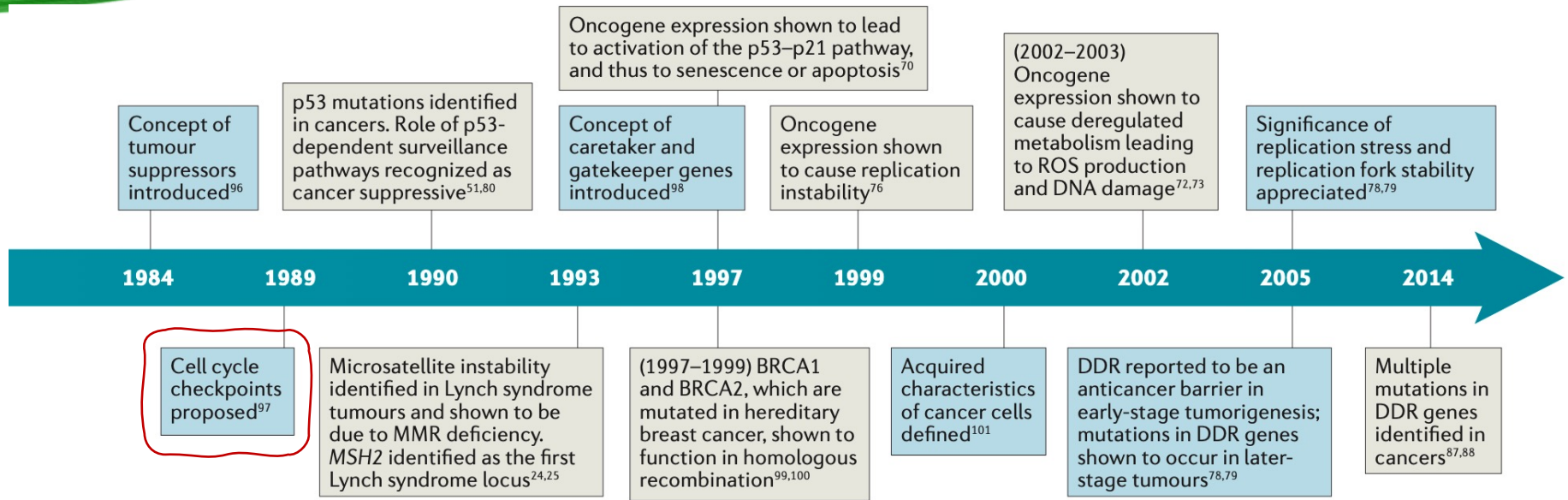
Il checkpoint da danni la DNA e l'arresto del ciclo cellulare



Bersagli del checkpoint



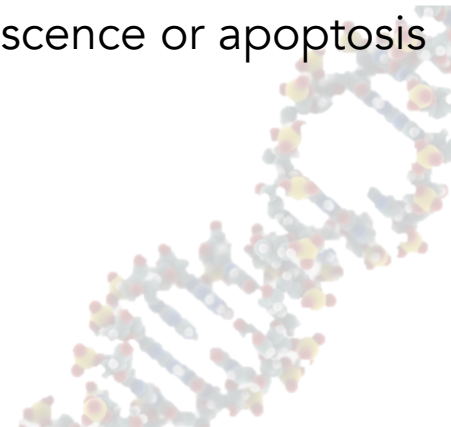
Instabilità genetica e danno al DNA



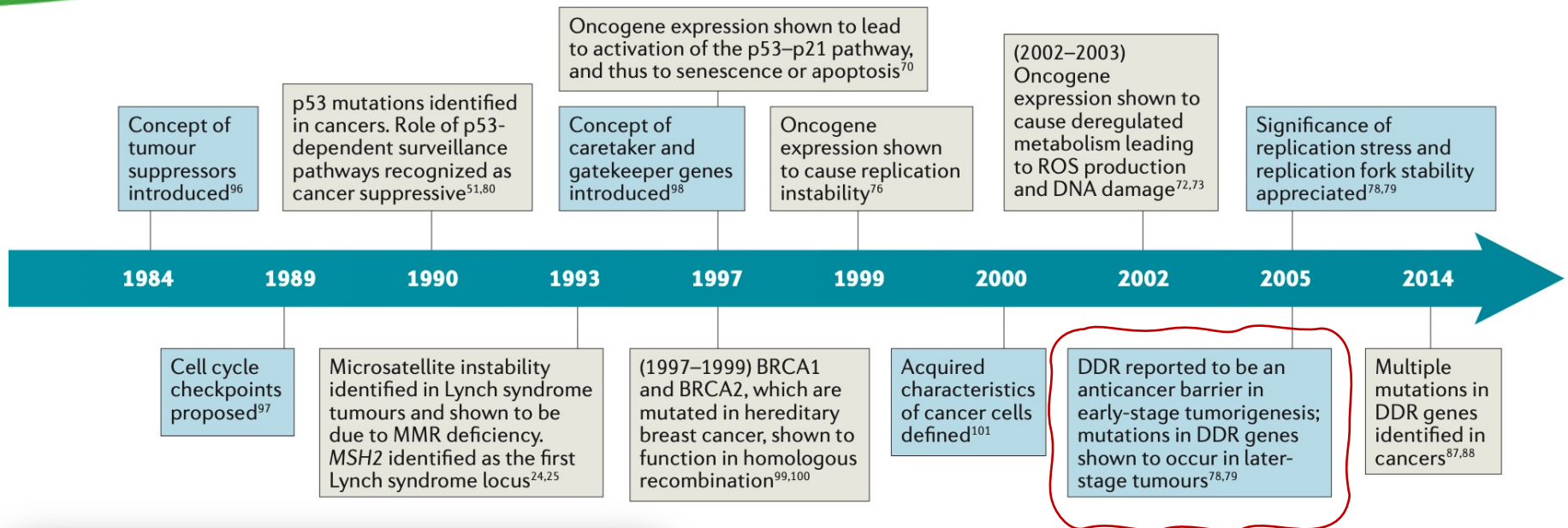
- ❖ 1990s: genome instability occurred rapidly after HRAS oncogene or other oncogenes expression
- ❖ Late 1990s: Oncogene-induced senescence and apoptosis
- ❖ 2000: DNA damage activated the p53–p21 pathway to drive senescence or apoptosis
→ IDEA: oncogene expression caused DNA damage

Oncogene expression → DNA damage? → CANCER?

When genome instability arises during cancer development?



Instabilità genetica e danno al DNA



Activation of the DNA damage checkpoint and genomic instability in human precancerous lesions

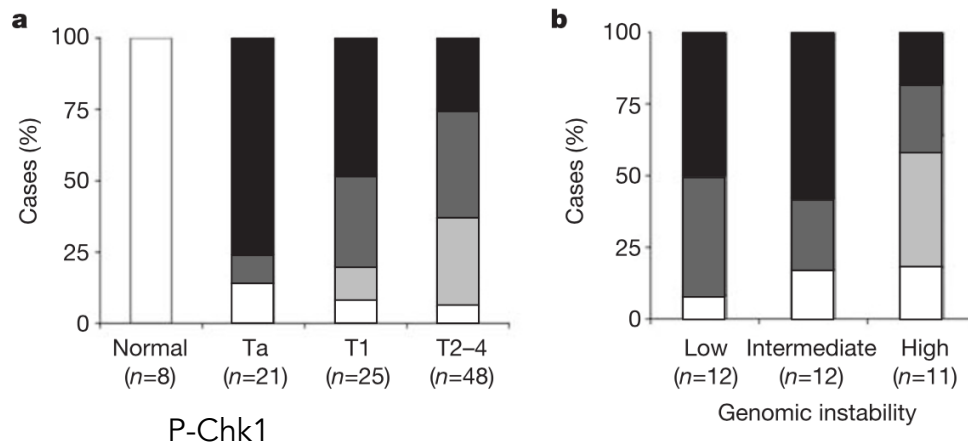
Vassilis G. Gorgoulis^{1*}, Leandros-Vassilios F. Vassiliou^{1*}, Panagiotis Karakaidos¹, Panayotis Zacharatos¹, Athanassios Kotsinas¹, Triantafillos Liloglou², Monica Venere^{3,4}, Richard A. DiTullio Jr^{3,4}, Nikolaos G. Kastrinakis¹, Brynn Levy⁶, Dimitris Kletsas⁷, Akihiro Yoneta³, Meenhard Herlyn³, Christos Kittas¹ & Thanos D. Halazonetis^{3,5}

DNA damage response as a candidate anti-cancer barrier in early human tumorigenesis

Jirina Bartkova¹, Zuzana Hořejší^{1,5}, Karen Koed², Alwin Krämer¹, Frederic Tort¹, Karsten Zieger², Per Guldberg¹, Maxwell Sehested³, Jahn M. Nesland⁴, Claudia Lukas¹, Torben Ørntoft², Jiri Lukas¹ & Jiri Bartek¹

Attivazione DDR in tumori a diversi stadi di sviluppo

- ❖ Ta: early superficial lesions
- ❖ T1: earliest invasive carcinomas
- ❖ T2–4: advanced primary carcinomas



Bianco: no P
Grigio: P

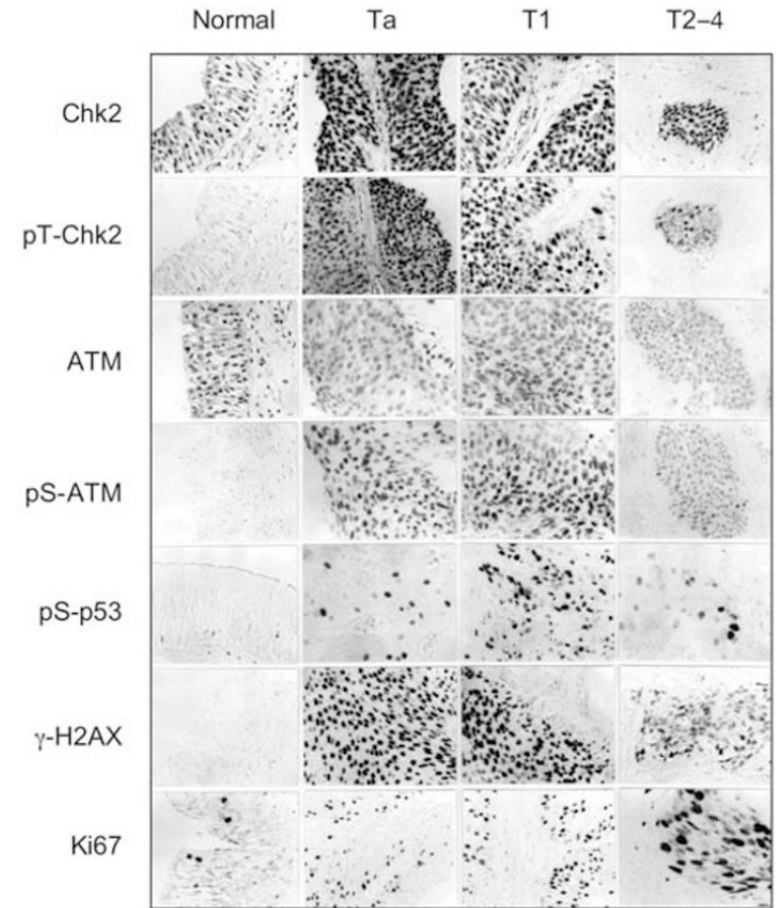
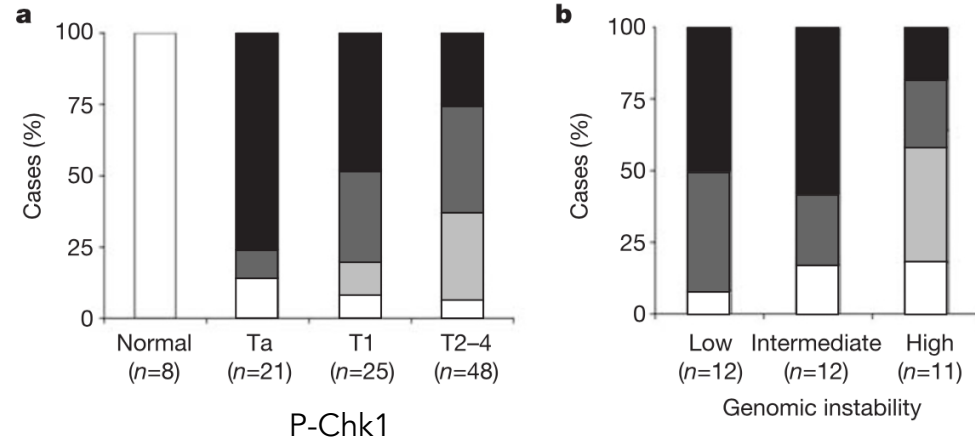


Figure 1 Constitutive activation of the ATM–Chk2–p53 pathway in human urinary bladder cancer. Immunohistochemistry of normal uroepithelium, early superficial lesions (Ta), earliest invasive (T1) and more advanced primary carcinomas (T2–4). Chk2 and ATM proteins are ubiquitously expressed, but Thr 68-phosphorylated Chk2 (pT-Chk2), Ser 1981-phosphorylated ATM (pS-ATM), Ser 15-phosphorylated p53 (pS-p53) and Ser 139-phosphorylated histone H2AX (γ-H2AX) are detectable only in tumour tissues. They are all present at the early stages of tumour development. Ki67 is a marker of proliferating cells. Original magnification, ×100.

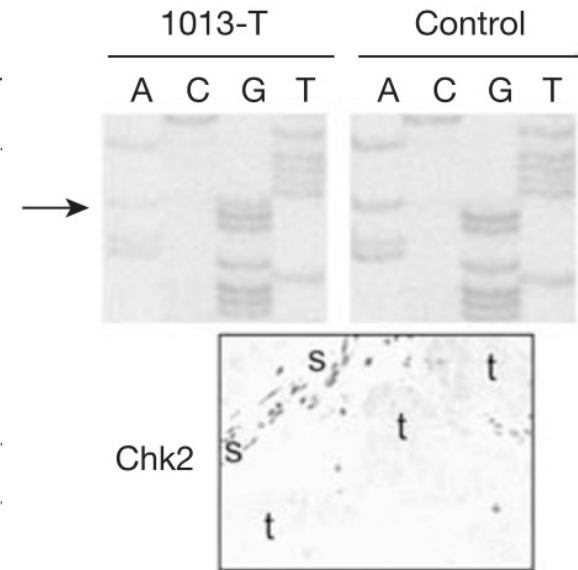
Attivazione DDR in tumori a diversi stadi di sviluppo

- ❖ Ta: early superficial lesions
- ❖ T1: earliest invasive carcinomas
- ❖ T2-4: advanced primary carcinomas

Bianco: no P
Grigio: P



Defects	Instability:		
	Low (n=12)	Intermediate (n=12)	High (n=11)
p53 mutation	0	1	6
p53 LOH	1	2	10
Chk2 mutation	0	1	1
Chk2 LOH	0	0	2
ATM LOH	0	4	3
ATM protein	0	0	2
Total	1	8	24



Risultati simili su altri tumori

Attivazione DDR nei tumori

Che cosa attiva DDR nel tumore?

cyclin E overexpression?

- common in carcinomas
- enhance genomic instability

U-2-OS-derived cells

Cyclin E repressed by Tet

